Available online at www.sciencedirect.com
SCIENCE DIRECT
Journal of Magnetic Resonance 180 (2006) 203–209
JMR Journal of Magnetic Resonance
www.elsevier.com/locate/jmr

Three-dimensional correlated accordion NMR spectroscopy of proteins

Keyang Ding *, Sujay Ithychanda, Jun Qin *

Structural Biology Program, Department of Molecular Cardiology, NB-20, Lerner Research Institute, the Cleveland Clinic Foundation, 9500 Euclid Avenue, Cleveland, OH 44195, USA

Received 8 January 2006; revised 7 February 2006
Available online 10 March 2006

Abstract

A major step toward the protein structure determination by nuclear magnetic resonance (NMR) spectroscopy is the assignment of multidimensional NMR signals that provide through-bond and through-space inter-atomic correlations. Ambiguities often occur during the assignment process due to resonance degeneracy, which challenges high resolution and larger size protein structure determination. Here, we present a method that will significantly improve the efficiency and accuracy of the NMR signal assignment. The method is based on a correlated accordion principle that, when incorporated into conventional three-dimensional (3D) heteronuclear NMR experiments, allows the retrieval of additional frequency correlation information at high resolution. We show that 3D spectra derived from this method are as effective as the impractical high resolution four-dimensional (4D) spectra with substantially reduced signal ambiguity as compared to their conventional counterparts. The approach promises increased accuracy and size of protein structures determined by NMR.

Keywords: Correlated accordion principle; Parallel correlation; NMR; Protein structure

1. Introduction

Contributing to nearly 20% of total 3D protein structures deposited in Protein Data Bank (PDB), NMR is widely recognized as one of the major tools for genomic/proteomic structural analyses as well as for molecular elucidation of a variety of fundamental biological processes. Compared to its rival X-ray crystallography, NMR offers a number of unique advantages such as determining protein structures in near physiological solution condition without the need for crystallization, probing mechanisms of protein dynamics/folding, and detecting weak transient protein-target interactions, etc. However, NMR-based protein studies suffer from two major limitations: (i) molecular size-dependent line broadening that leads to the loss of NMR signals, and (ii) resonance degeneracy that prevents unambiguous assignment of the signals. While the former could be alleviated by partial/full deuteration of proteins[1] and TROSY technique[2], the latter is often more problematic especially for the side-chain related signals despite the use of multidimensional approach and high field magnets. Since side chains are critically involved in the formation of protein tertiary fold and protein–target interactions, the ambiguity of their assignments presents a major challenge for high resolution and larger size protein structure determination by NMR.

Conventional protocol for protein structure determination by NMR involves two types of multidimensional heteronuclear experiments: (a) through-bond correlation experiments for obtaining resonance assignment and *J*-coupling-based dihedral angles; (b) through-space correlation experiments for obtaining ^{1}H–^{1}H distance constraints (<5 Å). In addition, residual dipolar coupling measurements provide some valuable long-range structural information[3,4]. These experiments are typically performed in ^{15}N- or ^{13}C-edited 3D fashions on $^{15}N/^{13}C$-labeled proteins. High resolution protein structure determination requires complete and unambiguous assignment for

* Corresponding authors. Fax: +1 216 445 1466.
E-mail addresses: dingk@ccf.org (K. Ding), qinj@ccf.org (J. Qin).

1090-7807/$ - see front matter © 2006 Elsevier Inc. All rights reserved.
doi:10.1016/j.jmr.2006.02.012

both through-bond and through-space correlations. However, resonance degeneracy often occurs even for small-medium sized proteins, which leads to ambiguity for the assignment especially for the side-chain-involved NOEs. Accumulation of the ambiguous assignments is the major cause for false or poor resolution structures determined by NMR. Theoretically, 4D experiments can provide dramatic resolution enhancement by extending another correlation into the fourth dimension[5–7], however, their conventional versions are less informative especially for the side-chain signals due to low digital resolution afforded by the limited experimental time. To reach high enough digital resolution for a 4D experiment as its corresponding 3D counterpart (normally 2–3 days), it would require 2–3 weeks, which is extremely time-consuming and costly. In reality, considering that many proteins have limited sample stability and that NMR instruments often require maintenance every 7–10 days, the high (digital) resolution 4D experiments are nearly impractical and therefore they have been seldom used in routine NMR protein structure determination. A variety of methods [8–14] have been developed recently to speed up the high dimensionality experiments such as non-linear sampling, spatially encoded NMR, SOFAST method, GFT method, and projection–reconstruction.

In this paper, we present a new set of 3D through-bond and through-space triple resonance correlation experiments by introducing a so-called correlated accordion principle. We show that these 3D experiments not only allow rapid data acquisition (collected in a matter of 1–2 days per experiment) but are remarkably effective in resolving signal ambiguities as compared to their conventional 3D counterparts, and the information obtained is equivalent to the hypothetical high digital resolution 4D counterparts. This new reduced dimensionality approach is particularly effective for resolving the side-chain degeneracy, which should dramatically improve the capacity of NMR in high resolution structural analyses of proteins and protein complexes and may further extend the size limit by NMR.

2. Overview of conventional triple resonance correlation experiments

Based on the type of magnetization transfer, the correlation between two spin systems can be classified as being either sequential or parallel. Sequential correlation is characteristic of through-bond connectivity, which is used for all triple resonance experiments during the protein backbone assignment. The magnetization transfer of such correlation is uniquely controlled by the combined use of forward and backward INEPTs via a number of relay spin systems. An example of sequential correlation is to connect the backbone chain H^N–^{15}N–^{13}CO– $^{13}C^{\alpha}$–H^{α} units in proteins. If there is no degeneracy in 2D ^{15}N–^{1}H HSQC, the five correlated chemical shifts for each H^N–^{15}N–^{13}CO–$^{13}C^{\alpha}$–H^{α} chain unit in a protein can be exclusively obtained from a hierarchy of three 3D triple resonance NMR spectra (for review of the conventional triple resonance experiments, see ref 15): HNCO, HN(CO)CA, and HN(COCA)HA or HA(CACO)NH. If there is some chemical shift degeneracy in 2D ^{15}N–^{1}H HSQC, addition of more 3D spectra such as H(N)COCA, H(N)CO(CA)HA, and H(NCO)CAHA to the hierarchy typically resolve the ambiguity problem. With five spin correlation H^N–^{15}N–^{13}CO–$^{13}C^{\alpha}$–H^{α} identified for all backbone units, their sequential correlations can be obtained from the 3D spectra that provide both intra and inter-residue $^{13}C^{\alpha}/H^{\alpha}$ correlations: HNCA, HA(CA)NH. If there is $^{13}C^{\alpha}/H^{\alpha}$ degeneracy, HNCACB and CBCACONH can be performed to obtain additional intra and inter-residue $^{13}C^{\beta}$ correlations that may resolve the ambiguity problem. This constitutes a common strategy for protein backbone resonance assignment by using sequential correlation-based triple resonance experiments.

In parallel correlation, the magnetizations of a number of spin systems are transferred simultaneously to a single spin system and/or vice versa. Generally, the parallel correlation is originated from the magnetization transfer through NOE (through-space) or HOHAHA (through-bond) mixing process. HCCH-NOESY, HCCH-TOCSY, HCNH-NOESY, HC(CCO)NH, and HNNH-NOESY are typical examples of parallel-correlated experiments in proteins. For convenience, these experiments are denoted as HMXH-type experiment. In contrast to sequential-correlated experiments, the four correlated chemical shifts for HMXH cannot be exclusively obtained from the following three 3D spectra: H(M)XH, (H)MXH, and HM(X)H. Although the symmetry property of HCCH or HNNH-type spectrum can help somewhat, the mismatching between H and M or X and H due to resonance degeneracy occurs quite frequently in routine 3D experiments, which leads to ambiguity in both side-chain resonance assignment as well as NOE-based assignment. Theoretically, 4D experiments such as HCCH-NOESY and HCNH-NOESY [5–7] would dramatically resolve the ambiguity problem. However, as mentioned in the introduction, 4D experiments are extremely time-consuming. In practice, 4D spectra are often poorly digitized within an affordable period of experimental time. This again leads to ambiguity problem. For example, the ^{1}H–^{13}C cross-peaks resolved in 2D ^{1}H–^{13}C HSQC spectrum may not be well resolved in 2D ^{1}H–^{13}C plane of the 4D spectrum.

3. The correlated accordion principle

The accordion principle [16,17] was proposed over 20 years ago for simultaneously observing a number of interactions in a common frequency dimension in multidimensional NMR experiments and has been used in various applications[18,19]. Along this common frequency dimension, the frequency of one interaction is detected quadraturely in the conventional way and the frequencies of the remaining interactions are observed as multiple splitting to the frequency detected quadraturely. By analyzing the splitting pattern along the common frequency dimension,

a number of frequencies can be obtained simultaneously. However, the introduced splitting decreases the resolution along the common frequency dimension. To recover the resolution along the common frequency dimension, two equivalent approaches were proposed. The first approach [20] employs the TPPI [21,22] that places cross-peaks within a splitting multiplet into respective non-overlapping regions along the common frequency dimension by introducing large artificial resonance offsets. The second approach [23,24] uses the IPAP in combination with interleaved data acquisition [25–27], which separate the cross-peaks within a splitting multiplet into different subspectra by iteratively combining the in-phase and anti-phase splitting. Both approaches suggest that the accordion principle may be applicable to triple-resonance experiments for sequential correlation. However, little is known about the applicability and power of the accordion principle in parallel correlated HMXH-type experiments, which may address the central degeneracy problem for side chain resonances and side-chain-related NOEs.

For convenience, the spin systems HM and XH in parallel-correlated HMXH-type experiments before and after the NOE or HOHAHA mixing period are called the initial spin systems and the destination spin systems. Based on the spin frequencies detected in the common frequency dimension, we can derive three schemes A, B, and C, which employ the accordion principle in HMXH-type experiments. The scheme A adopts $H(t_2)M(t_1)X(t_2)H(t_3)$ in the time domain, in which the initial H and the destination X are measured in a common dimension. The scheme B employs $H(t_1)M(t_2)X(t_2)H(t_3)$ in the time domain, where the initial M and the destination X are measured in a common dimension. The scheme C follows $H(t_2)M(t_2)X(t_1)H(t_3)$ in the time domain, where the initial H and the initial M are measured in a common dimension. Detailed analysis below indicates that these three schemes belong to two distinct classes that can lead to dramatically different results. The schemes A and B belong to the class of correlated accordion that requires that an initial spin and a destination spin be measured in a common frequency dimension. In contrast, the scheme C does not have the above requirement and is thus called uncorrelated accordion method.

Fig. 1A schematically shows the spectrum of HCCH-type experiment by using the scheme A where the initial ^{13}C is used as the editing dimension (F_1), the initial ^{1}H split

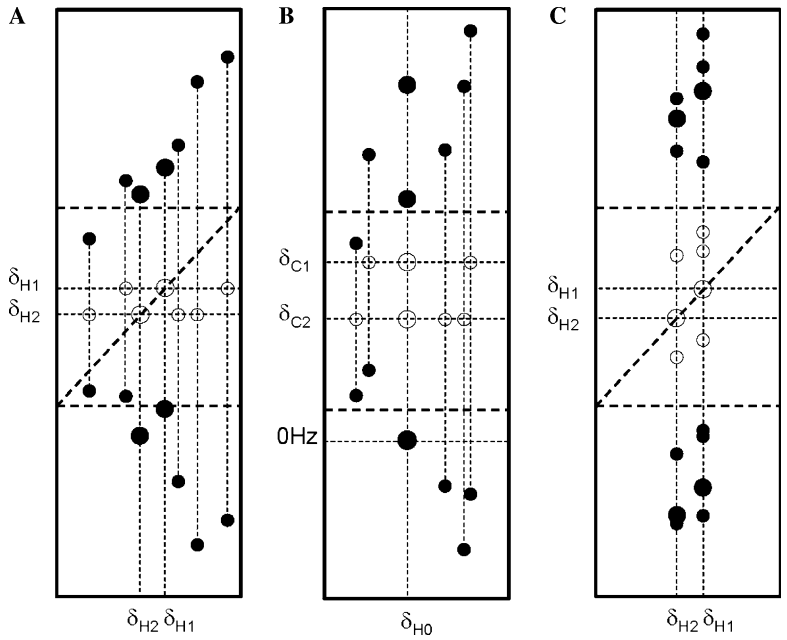

Fig. 1. Schematic representation of the correlated accordion principle (A) or (B) versus uncorrelated accordion method (C). Both (A and B) for 3D HCCH-type experiment require that (i) either initial ^{13}C or initial ^{1}H should be used as the editing dimension (F_1); (ii) either initial ^{1}H or initial ^{13}C split by the destination ^{13}C should be detected quadraturely in the correlated accordion dimension (F_2); and (iii) the destination ^{1}H is directly detected in real time (F_3). In both (A and B), the 2D F_3F_2-planes intersecting to F_1 at δ_{C0} or δ_{H0} are shown where the filled cycles represent the cross-peaks from 3D correlated accordion HCCH spectrum and the open cycles represent the cross-peaks from the conventional 3D HC(C)H spectrum. TPPI is applied to the destination ^{13}C to create a large artificial resonance offset. The diagonal peak doublets in (A) are centered on the diagonal line and the splitting for all diagonal peaks present in the same 2D plane should be the same and equal to the frequency of the initial ^{13}C relative to the TPPI-shifted carrier. The diagonal peak doublets in (B) are located on a line parallel to F_2 dimension and intersecting F_3 at δ_{H0} and the low-field peaks from all the diagonal peak doublets coincide at the TPPI-shifted 0Hz line. For the uncorrelated accordion method (C), the destination ^{13}C is used as the editing dimension (F_1), the initial ^{1}H split by the initial ^{13}C is quadraturely detected in F_2 dimension and the destination ^{1}H is directly detected in real time (F_3). TPPI is applied to the initial ^{13}C to create a large artificial resonance offset. The 2D F_3F_2-plane intersecting to F_1 at δ_{C0} is shown where the filled cycles represent the cross-peaks from 3D uncorrelated accordion HCCH spectrum and the open cycles represent the cross-peaks from the conventional 3D H(C)CH spectrum. The diagonal peak doublets in (C) are centered on the diagonal line and the splitting for all diagonal peaks present in the same 2D plane should be the same and equal to the frequency of the initial ^{13}C relative to the TPPI-shifted carrier.

by the destination ^{13}C is quadraturely detected in the correlated accordion dimension (F_2) and the destination ^{1}H is directly detected in the real-time dimension (F_3). TPPI on the destination ^{13}C is used to place the splitting peaks into two non-overlapping regions. In a 2D plane (F_3F_2) intersecting to F_1 at δ_{C0}, the cross-peaks originated from two initial CHs (δ_{H1}, δ_{C0}) and (δ_{H2}, δ_{C0}) are assumed to be present. The filled cycles represent the cross-peaks from the correlated accordion 3D HCCH spectrum, while the open cycles represent the cross-peaks from the conventional 3D HC(C)H spectrum. Careful examination of this 3D correlated accordion spectrum reveals three features. First of all, the splitting direction is perpendicular to the correlation axis. It is obvious that the conventional 3D HC(C)H spectrum provides the center positions for the splitting pairs in the correlated accordion 3D HCCH spectrum. In the conventional 3D HC(C)H spectrum, all the cross-peaks (the diagonal peak and the off-diagonal peaks) arisen from an individual initial CH are, according to δ_H of the initial ^{1}H, co-axially located along a line that can be called the correlation axis. Since the splitting direction and the correlation axis are perpendicular, the resolution of the correlated accordion spectrum is clearly better than its conventional 3D HC(C)H spectrum. Strikingly, this co-axial property of the splitting pairs could be used to pair the split peaks without the need of its conventional 3D HC(C)H for measuring the center positions. For the diagonal peaks, the splitting pair for each initial CH should be centered on the diagonal line and the splitting for all the diagonal peaks present in the same 2D plane should be the same and equal to the sum of the frequency of initial ^{13}C relative to the carrier. The diagonal peak pairs can be used to identify the correlation axis.

The 3D correlated accordion HCCH experiment by using scheme B is schematically depicted in Fig. 1B, in which the initial ^{1}H is used as the editing dimension (F_1), the initial ^{13}C split by the destination ^{13}C is quadraturely detected in the correlated accordion dimension (F_2) and the destination ^{1}H is directly detected in the real-time dimension (F_3). TPPI on the initial ^{13}C is used to place the splitting peaks into two non-overlapping regions. Comparison with Fig. 1A reveals different features where the correlation axis is labeled by δ_C of the initial ^{13}C and all the diagonal peak pairs are located on the same line perpendicular to the correlation axis and labeled by δ_H of the initial ^{1}H. Note that the open cycles in Fig. 1B still represent the cross-peaks from the conventional 3D HC(C)H spectrum.

For uncorrelated accordion method (the scheme C), the destination ^{13}C is used as the editing dimension (F_1), the initial ^{1}H split by the initial ^{13}C is quadraturely detected in the uncorrelated accordion dimension (F_2) and the destination ^{1}H is directly detected in the real-time dimension (F_3). The resulting spectrum is schematically shown in Fig. 1C. The open cycles represent the cross-peaks from the conventional 3D H(C)CH spectrum. The uncorrelated accordion method has been explored recently[13,26,27], however, its resolution, as shown in Fig. 1C, remains essentially the same as its conventional 3D H(C)CH spectrum. Further, different from the schemes A and B, it needs the conventional 3D H(C)CH spectrum to measure the center positions for the splitting pairs and otherwise, and hence is very difficult to correctly pair the splitting peaks.

It should be noted that by using TPPI, the splitting doublets are positioned into two non-overlapping regions in 3D space (Fig. 1A) while the total number of peaks present in each region is the same as in the conventional 3D spectrum. Although one can expand the whole spectrum into two sub-spectra, they may be better maintained in the same spectrum for ready analysis since they are not overlapping. As mentioned above, the separation of the splitting doublet can be also achieved by IPAP technique with interleaved acquisition, although both TPPI and IPAP would lead to the same resolution and sensitivity with the same experimental time. TPPI-90 and IPAP/GFT are equivalent. However, if using non-90, TPPI takes less time than IPAP/GFT. The TPPI results can be converted to the IPAP results by simply expanding the whole 3D spectrum, however, the IPAP subspectra are not easily used to compose the whole spectrum of TPPI result. To manually view the spectrum to find out the co-axis, the TPPI result would be better. It should also be noted that for HCNH-type experiments, no diagonal peak pairs can be used to identify the correlation axis. However, additional spectrum to measure the center position is not necessary in this case since the co-axial property can be also used to elucidate the correlation of the four chemical shifts (^{1}H, ^{15}N, ^{13}C, ^{1}H) by comparison with the ^{15}N frequency measured from 2D ^{15}N–^{1}H HSQC spectrum.

4. Results and discussion

By employing the correlated accordion principle, we have designed a set of through-bond and through-space 3D experiments including HCCH-NOESY, HCNH-NOESY, HNNH-NOESY, HCCH-TOCSY, HC(CCO)NH, $H_{\alpha\beta}C_{\alpha\beta}$(CO)NH and $H_{\alpha\beta}C_{\alpha\beta}$NH. These experiments correspond to conventional[15] 4D ^{13}C/^{13}C-edited NOESY, 4D ^{13}C/^{15}N-edited NOESY, 4D ^{15}N/^{15}N-edited NOESY, 3D HCCH-TOCSY, 3D CCONH/HCCONH, 3D CBCACONH/HBHACONH, and CBCANH/HBHANH respectively. Of these new 3D experiments we have developed, the HCCH-NOESY, HCNH-NOESY, and HNNH-NOESY can retrieve all NOE-based proton–proton distance restraints that are vital for protein structure determination. The HCCH-TOCSY, HC(CCO)NH, $H_{\alpha\beta}C_{\alpha\beta}$(CO)NH can promote highly effective and unambiguous side chain resonance assignment. The $H_{\alpha\beta}C_{\alpha\beta}$(CO)NH and $H_{\alpha\beta}C_{\alpha\beta}$NH can be used for backbone resonance assignment. The detailed pulse sequences and their description for the proposed experiments are provided in the supplementary material. Every sequence has been tested and the data were collected on protein samples in comparison with their corresponding conventional sequences. Here, we use

HCCH-NOESY as an example to illustrate the power of the correlated accordion method as compared to its corresponding counterparts. The incorporation of the method (Scheme A in Fig. 1) is very straightforward as shown in Fig. 2. To make a meaningful comparison, we have first collected the conventional 3D and 4D HCCH-NOESY using a protein complex (15 kDa) between filamin repeat 21 (FLN-21, 12.5 kDa) and the N-terminal fragment of migfilin (migfilin-N 2.5 kDa), which have been shown to be involved in focal adhesions [28]. One millimolar $^{15}N/^{13}C$-labeled FLN-21 was mixed with 1.3 mM unlabled migfilin-N in 40 mM phosphate buffer, 10 mM NaCl, pH 6.5 for the NMR experiments. Fig. 3A shows a selected region in $F_3(^1H)$–F_2- (^{13}C, 18.5 ppm) plane at F_1 (^1H, 0.55 ppm) of the conventional HCCH-NOESY spectrum. The strip reveals potential NOE contacts from the FLN-21 V105 $C^{\gamma 1}H_3$ (^1H-0.55 ppm, ^{13}C-18.5 ppm) to the neighboring protons, however, because V105 $C^{\gamma 1}H_3$ is very close to several other methyl groups, the assignment of the NOEs was difficult even if we used the symmetry properties of the peaks. This situation was improved in the conventional 4D HCCH-NOESY (Fig. 3B) where we were able to distinguish one NOE to A33 $C^{\alpha}H$ from other well-resolved NOEs that belong to methyls of other residues (see the label). However, due to poor digital resolution at ^{13}C dimension, it was impossible to distinguish NOEs in the circled region. Fig. 3C shows the 3D correlated accordion NOESY spectrum, which corresponds to the same region in Fig. 3B. The spectral resolution is clearly dramatically better than Fig. 3B, which led to the straightforward assignment of the NOE peak V105 $C^{\gamma 1}H_3$/V105 $C^{\alpha}H$ and a long range NOE peak V105 $C^{\gamma 1}H_3$/V32 $C^{\alpha}H$ (see labels). Other remaining NOE peaks were easily determined to be from other planes based on their intensities, which belong to other methyls. It should be noted that when multiple peaks are resolved along the F2-dimension (^{13}C) but not along the F3-dimension (^1H), the correlated accordion method is very powerful to make the precise determination of which peaks are paired in the two subspectra (see the arrows in Fig. 3D).

The improvement of 3D correlated accordion spectrum as compared to the corresponding conventional 3D counterpart is most evident, as the former not only increased the correlation content, but also substantially increased the resolution (Fig. 3C vs Fig. 3A). As shown above, the improvement is also dramatic as compared to the conventional 4D experiment. Calculation indicated that to reach the same resolution as our 3D correlated accordion HCCH-NOESY that took 2 days, it would take at least two weeks of experimental time, which is extremely time consuming and impractical. By using the correlated accordion principle, our new 3D HCCH-NOESY is essentially equivalent to a high resolution 4D NOESY, which reflects a quantum jump in our ability to analyze the multidimensional NMR spectra. This is especially significant for assignment of the long range methyl to methyl NOEs that play critical roles in protein tertiary fold and protein–protein interfaces. For example, the methyl–methyl NOE cross-peaks are often close to the strong diagonal peaks in the conventional 4D HCCH-NOESY. Although it is possible to suppress the diagonal peaks[29], it would double the experimental time[29]. To extend the above calculation, suppression of the diagonal peaks would take at least 4 weeks for the 4D HCCH-NOESY to reach the same resolution as the 3D correlated accordion HCCH-NOESY that would only take 4 days. The former is impossible yet the latter is very feasible, which would lead to unambiguous assignment of many critical methyl-methyl NOEs.

The effectiveness of the correlated accordion method is also evident in the through-bond triple resonance experiments. For example, a single correlated accordion HC(CCO)NH experiment can replace the conventional C(CCO)NH and H(CCO)NH experiments that are used for assigning ^1H and ^{13}C resonances respectively. Remarkably, the former directly correlates the ^1H resonance(s) to its attached ^{13}C whereas the latter are two independent experiments that do not provide such direct correlation.

In summary, we have developed a suite of new 3D through-bond and through-space 3D experiments using a

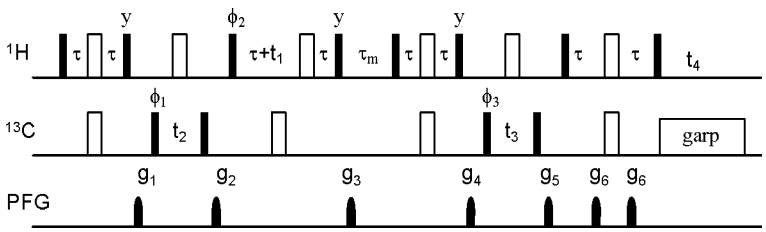

Fig. 2. Schematic representation of HCCH-NOESY pulse sequence. The filled and open bars represent 90° and 180° pulses with phase x, respectively, unless indicated otherwise. The carrier frequency for ^1H is at 2.5 ppm before the last INEPT or 4.7 ppm at the beginning of the last INEPT. The carrier frequency for ^{13}C is 43 ppm. The inter-pulse delays are $\tau = 1.65$ ms and $\alpha = 1$ ms, respectively. The NOE mixing time τ_m is 150 ms. The phase cycles are as follows: $\phi_1 = x,-x$; $\phi_2 = x$; $\phi_3 = x, x, -x, -x$; $\phi_{Rec} = x, -x, -x, x$. The PFG g_1, g_2, g_3, g_4 and g_5 are applied at $z$direction with maximal 20 G/cm with different shapes and durations, respectively, to avoid any proportionality and the PFG g_6 is applied at z-direction with maximal 20 G/cm with duration of 0.6 ms. The reference spectrum[29] for suppressing NOE diagonal peaks is recorded in the interleaved manner by implementing $2H_zC_z$ evolution during the NOE mixing period. For correlated accordion 3D experiment: $t_2 = t_3$; the phases ϕ_1 and ϕ_2 are incremented in the States-TPPI manner for quadrature detection in F_1 and F_2 dimensions. The phase ϕ_3 is incremented in the TPPI manner for introducing an artificial offset. For conventional 3D experiment: $t_3 = 0$; the phases ϕ_1 and ϕ_2 are incremented in the States-TPPI manner for quadrature detection in F_1 and F_2 dimensions. For conventional 4D experiment: the phases ϕ_1, ϕ_2, and ϕ_3 are incremented in the States-TPPI manner for quadrature detection in the F_1, F_2, and F_3 dimensions. Note that the HSQC-version instead of HMQC-version is employed since the former can be used to better suppress the water suppression.

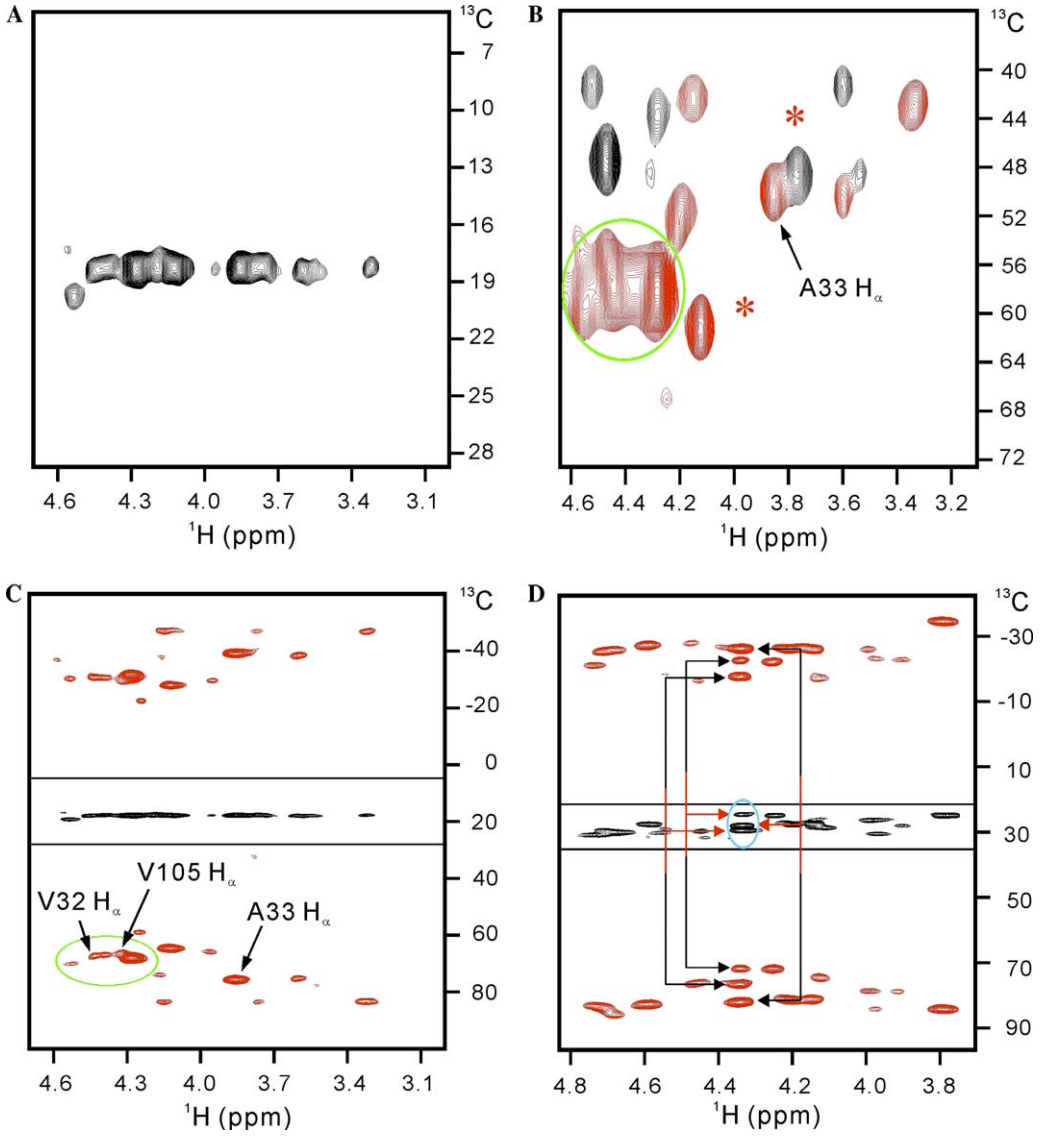

Fig. 3. Selective regions of HCCH-NOESY spectra measured on 1 mM FLN-21 in complex with migfilin-N in 40 mM phosphate buffer, 10 mM NaCl, pH 6.5, 29 °C. (A) The 2D F_3F_2-plane at 0.55 ppm (^{1}H-F$_1$) taken from the conventional 3D spectrum. Data points are 64* (^{1}H-F_1) × 64* (^{13}C- F_2) × 512* (^{1}H-F_1) and the corresponding spectral width is 4255.319 Hz(^{1}H-F_1) × 10593.221 Hz(^{13}C-F_2) × 8992.806 Hz(^{1}H-F_3). Total experimental time: one day. (B) 2D F_4F_3-plane at 0.55 ppm (^{1}H-F_1) and 18.5 ppm (^{13}C-F_2) taken from the conventional 4D spectrum. A very crowded spectral region is circled by green, however, compared to (A), some peaks are well resolved, e.g., a long range NOE between V105 C$^\gamma$H$_3$ and A33 C$^\alpha$H. Data points are 22* (^{1}H-F_1) × 20* (^{13}C-F_2) × 20* (^{13}C-F_3) × 512* (^{1}H-F_4) and the corresponding spectral width is 4255.319(^{1}H-F_1) × 10593. 221(^{13}C-F_2) × 10593. 221(^{13}C-F_3) × 8992. 806(^{1}H-F_4). Total experimental time: 4 days. Note that the residual peaks from its neighboring planes, due to low digital resolutions in F_1 and F_2 dimensions, are indicated as black. Asterisk (*) indicates peaks seen at lower contour level. (C) The 2D F_3F_2-plane at 0.55 ppm (^{1}H–F$_1$) taken from correlated accordion 3D spectrum. The spectrum in (A) is inserted in the black box for comparison. The same region circled in (B) (green) is also circled by green. Dramatic improvement in resolution in (C) can be seen as compared to (B) (see the circled regions), which allow unambiguous assignment of some important long range NOE, e.g., V105 C$^\gamma$H$_3$ and V32 C$^\alpha$H (see the label). Data points are 64* (^{1}H-F_1) × 128* (^{13}C-F_2) × 512* (^{1}H-F_3) and the spectral width 4255.319(^{1}H-F_1) × 42372. 884(^{13}C-F_2) × 8992. 806(^{1}H-F_3). Total experimental time: 2 days. The formula to calculate the ^{13}C chemical shifts of a peak are: $\Omega_{C1} = (\Omega_I + \Omega_{II})/2$ for the ^{13}C attached to ^{1}H at 0.55 ppm and $\Omega_{C2} = O_{r.f.} - [(\Omega_{II} - \Omega_I)/2 - SW_2/4]$ for the ^{13}C attached to ^{1}H that gives NOE to the ^{1}H at 0.55 ppm. Ω_I and Ω_{II} are the chemical shifts of a pair of peaks in the upper and lower half of the spectrum, $O_{r.f.}$ is the carrier frequency for ^{13}C, and SW_2 is the spectral width in the ^{13}C dimension. (D) The 2D F_3F_2-plane at 1.9 ppm (^{1}H-F_1) taken from the correlated accordion 3D spectrum illustrating how the degenerate 1H peaks can be resolved by ^{13}C using the correlated accordion method. For comparison, the same plane in the corresponding conventional 3D spectrum is inserted at the black box position. The peak pairing for three δ_H-degenerate peaks via ^{13}C frequencies is shown by arrows. Note that the center peaks circled by blue are also measured in the same 2D plane as the diagonal peaks in the correlated accordion 3D spectrum.

novel correlated accordion principle. Our data show that the new experiments provide dramatically improved resolution as compared to their conventional 3D/4D counterparts. These new 3D experiments are in principle as effective as the high digital resolution 4D experiments that are practically impossible due to extremely long acquisition times. Our new method not only provides a cost-effective approach for high-throughput proteomics/genomics but

also makes it possible for very high resolution structural studies of proteins. The correlated accordion principle can be also extended to modify experiments for very large proteins such as the methyl HCCH-NOESY and the methyl-backbone HCNH-COSY.

Acknowledgment

This work was financially supported by NIH Grants to J.Q.

Appendix A. Supplementary data

Supplementary data associated with this article can be found, in the online version, at doi:10.1016/j.jmr.2006.02.012.

References

[1] K.H. Gardner, L.E. Kay, The use of H-2, C-13, N-15 multidimensional NMR to study the structure and dynamics of proteins, Annu. Rev. Biophys. Biomol. Struct. 27 (1998) 357–406.
[2] K. Pervushin, R. Riek, G. Wider, K. Wuthrich, Attenuated T-2 relaxation by mutual cancellation of dipole–dipole coupling and chemical shift anisotropy indicates an avenue to NMR structures of very large biological macromolecules in solution, Proc. Natl. Acad. Sci. USA 94 (1997) 12366–12371.
[3] J.R. Tolman, J.M. Flanagan, M.A. Kennedy, J.H. Prestegard, Nuclear magnetic dipole interactions in field-oriented proteins—information for structure determination in solution, Proc. Natl. Acad. Sci. USA 92 (1995) 9279–9283.
[4] N. Tjandra, A. Bax, Direct measurement of distances and angles in biomolecules by NMR in a dilute liquid crystalline medium, Science 278 (1997) 1111–1114.
[5] L.E. Kay, G.M. Clore, A. Bax, A.M. Gronenborn, Four-dimensional heteronuclear triple-resonance NMR-spectroscopy of interleukin-1-beta in solution, Science 249 (1990) 411–414.
[6] G.M. Clore, L.E. Kay, A. Bax, A.M. Gronenborn, Four-dimensional C-13/C-13-edited nuclear Overhauser enhancement spectroscopy of a protein in solution—application to interleukin 1-beta, Biochemistry 30 (1991) 12–18.
[7] G.M. Clore, A.M. Gronenborn, Structures of larger proteins in solution—3-dimensional and 4-dimensional heteronuclear NMR-spectroscopy, Science 252 (1991) 1390–1399.
[8] D. Marion, Fast acquisition of NMR spectra using Fourier transform of non-equispaced data, J. Biomol. NMR. 32 (2) (2005) 141–150.
[9] Y. Shrot, L. Frydman, Spatially encoded NMR and the acquisition of 2D magnetic resonance images within a single scan, J. Magn. Reson. 172(2) 179–190.
[10] P. Schanda, E. Kupce, B. Brutscher, SOFAST-HMQC experiments for recording two-dimensional deteronuclear correlation spectra of proteins within a few seconds, J. Biomol. NMR. 33 (4) (2005) 199–211.
[11] S. Kim, T. Szyperski, GFT NMR, a new approach to rapidly obtain precise high-dimensional NMR spectral information, J. Am. Chem. Soc. 125 (2003) 1385–1393.
[12] E. Kupce, R. Freeman, Projection-reconstruction technique for speeding up multidimensional NMR spectroscopy, J. Am. Chem. Soc. 126 (20) (2004) 6429–6440.
[13] L. Jiang, B.E. Coggins, P. Zhou, Rapid assignment of protein side chain resonances using projection-reconstruction of (4,3)D HC(CCO)NH and intra-HC(C)NH experiments, J. Magn. Reson. 175 (2005) 170–176.
[14] K. Ding, A.M. Gronenborn, Novel 2D triple-resonance NMR experiments for sequential resonance assignments of proteins, J. Magn. Reson. 156 (2002) 262–268.
[15] A. Bax, S. Grzesiek, Methodological advances in protein NMR, Accounts Chem. Res. 26 (1993) 131–138.
[16] G. Bodenhausen, R.R. Ernst, The accordion experiment, a simple approach to 3-dimensional NMR-spectroscopy, J. Magn. Reson. 45 (1981) 367–373.
[17] G. Bodenhausen, R.R. Ernst, Direct determination of rate constants of slow dynamic processes by two-dimensional accordion spectroscopy in nuclear magnetic-resonance, J. Am. Chem. Soc. 104 (1982) 1304–1309.
[18] J.R. Tolman, J.H. Prestegard, Measurement of amide ^{15}N–^{1}H one-bond couplings in proteins using accordion heteronuclear-shift-correlation experiments, J. Magn. Reson. B. 112 (3) (1996) 269–274.
[19] P.A. Carr, D.A. Fearing, A.G. Palmer 3rd, 3D accordion spectroscopy for measuring ^{15}N and ^{13}CO relaxation rates in poorly resolved NMR spectra, J. Magn. Reson. 132 (1) (1998) 25–33.
[20] G. Drobny, A. Pines, S. Sinton, D. Weitekamp, D. Wemmer, Fourier transform multiple quantum nuclear magnetic resonance, Faraday Div. Chem. Soc. Symp. 13 (1979) 49–174.
[21] G. Bodenhausen, R.L. Vold, R.R. Vold, Multiple quantum spin–echo spectroscopy, J. Magn. Reson. 37 (1980) 93–106.
[22] W. Kozminski, I. Zhukov, Multiple quadrature detection in reduced dimensionality experiments, J. Biomol. NMR 26 (2003) 157–166.
[23] D. Yang, K. Nagayama, A sensitivity-enhanced method for measuring heteronuclear long-range coupling constants from the displacement of signals in two 1D subspectra, J. Magn. Reson. A118 (1996) 117–121.
[24] A. Meissner, J.O. Duus, O.W. Sorensen, Integration of spin-state-selective excitation into 2D NMR correlation experiments with heteronuclear ZQ/2Q pi rotations for (1)*J*(XH)-resolved E.COSY-type measurement of heteronuclear coupling constants in proteins, J. Biomol. NMR 10 (1997) 89–94.
[25] M. Ottiger, F. Delaglio, A. Bax, Measurement of *J* and dipolar couplings from simplified two-dimensional NMR spectra, J. Magn. Reson. 131 (1998) 373–378.
[26] Y. Shen, H.S. Atreya, G. Liu, T. Szyperski, G-matrix Fourier transform NOESY-based protocol for high-quality protein structure determination, J. Am. Chem. Soc. 127 (2005) 9085–9099.
[27] Z.Y.J. Sun, S.G. Hyberts, D. Rovnyak, S. Park, A.S. Stern, J.C. Hoch, G. Wagner, High-resolution aliphatic side-chain assignments in 3D HCcoNH experiments with joint H–C evolution and non-uniform sampling, J. Biomol. NMR 32 (2005) 55–60.
[28] Y. Tu, S. Wu, X. Shi, K. Chen, C. Wu, Migfilin and Mig-2 link focal adhesions to filamin and the actin cytoskeleton and function in cell shape modulation, Cell 113 (1) (2003) 37–47.
[29] J. Wu, J.S. Fan, S.M. Pascal, D.W. Yang, General method for suppression of diagonal peaks in heteronuclear-edited NOESY spectroscopy, J. Am. Chem. Soc. 126 (2004) 15018–15019.